

Acute hypoxia suppresses blood glycolysis in saker falcons (*Falco cherrug*) via NR3C1-mediated repression of *HK1*: Evidence from hematological and epigenomic profiling

Wei Wu^{1,2,3,4}, Xiao-Hang Zhang^{1,2,3,4}, Fei-Fei Du^{1,2,3}, Zhong-Ru Gu^{1,2,3}, Li Hu^{1,5}, Jun-Feng Chen^{1,2}, Zhen-Zhen Lin^{1,2,3}, Sheng-Kai Pan^{1,2,3,6,*}, Xiang-Jiang Zhan^{1,2,3,7,*}

¹ State Key Laboratory of Animal Biodiversity Conservation and Integrated Pest Management, Institute of Zoology, Chinese Academy of Sciences, Beijing 100101, China

² Key Laboratory of Animal Ecology and Conservation Biology, Institute of Zoology, Chinese Academy of Sciences, Beijing 100101, China

³ Cardiff University-Institute of Zoology Joint Laboratory for Biocomplexity Research, Chinese Academy of Sciences, Beijing 100101, China

⁴ University of the Chinese Academy of Sciences, Beijing 100049, China

⁵ Yantai Institute of Coastal Zone Research, Chinese Academy of Sciences, Yantai, Shandong 264003, China

⁶ School of Nature Conservation, Beijing Forestry University, Beijing 100083, China

⁷ Center for Excellence in Animal Evolution and Genetics, Chinese Academy of Sciences, Kunming, Yunnan 650201, China

ABSTRACT

Ongoing climate change is driving high-altitude bird species to occupy even higher elevations, yet physiological and regulatory responses enabling these transitions remain poorly understood. This study investigated acute hypoxic responses in saker falcons (*Falco cherrug*) inhabiting the Qinghai-Xizang Plateau by exposing individuals to simulated altitudes of 5 000–6 000 m above sea level (a.s.l.), exceeding their typical elevation range (approximately 4 300 m a.s.l.). GPS tracking data indicated that juvenile falcons maintained comparable activity levels across 4 000–5 000 m and 5 000–6 000 m a.s.l. ranges. However, pre-fledging individuals subjected to 6 000 m hypoxia for three days exhibited marked increases in hemoglobin concentration and blood glucose. Transcriptomic profiling revealed significant suppression of glycolytic activity, notably characterized by reduced expression of hexokinase 1 (*HK1*), a key enzymatic gene involved in the glycolytic pathway. ATAC-seq further identified enhanced chromatin accessibility within the *HK1* locus under hypoxia, revealing two conserved cis-regulatory elements recognized by the transcription factor NR3C1 in the hypoxia-treated group. NR3C1 expression was negatively correlated with *HK1*. Notably, both elements were unique and evolutionarily conserved in avian taxa, suggesting a potential role in hypoxia resilience

This is an open-access article distributed under the terms of the Creative Commons Attribution Non-Commercial License (<http://creativecommons.org/licenses/by-nc/4.0/>), which permits unrestricted non-commercial use, distribution, and reproduction in any medium, provided the original work is properly cited.

Copyright ©2025 Editorial Office of Zoological Research, Kunming Institute of Zoology, Chinese Academy of Sciences

among highland birds. These findings provide mechanistic insights into the molecular and physiological strategies employed by sakers to tolerate acute hypoxic stress and inform conservation efforts for high-altitude bird species on the Qinghai–Xizang Plateau and other alpine ecosystems facing accelerating climate change.

Keywords: Hypoxic response; Qinghai-Xizang Plateau; Saker falcons; Glycolysis; Climate change

INTRODUCTION

The Qinghai-Xizang Plateau, often referred to as the “Third Pole of the World”, presents one of the most extreme terrestrial environments on Earth, characterized by chronic hypoxia, low ambient temperatures, and intense ultraviolet radiation (Hu et al., 2022). Among these environmental pressures, reduced oxygen availability imposes the most severe constraint on resident organisms (Pan et al., 2017). Ongoing climate warming has driven an upslope shift in the elevational distribution of many bird species native to the plateau region (Jiang et al., 2023; Li et al., 2023; Meng et al., 2021), thereby exacerbating the intensity of hypoxic stress encountered at higher altitudes (Parmesan & Yohe, 2003). Despite these changes, the mechanisms by which birds respond to increasingly severe hypoxic conditions across short timescales remain largely unexplored.

Vertebrate stress responses to environmental change typically occur in two temporal phases: an acute response triggered within minutes to days, and a chronic phase that emerges under prolonged exposure (Collier & Gebremedhin, 2015; Ho et al., 2020). Acute hypoxia responses in birds

Received: 18 May 2025; Accepted: 22 July 2025; Online: 23 July 2025

Foundation items: This study was supported by the National Nature Science Foundation of China (32222012, 32125005, 32270455, 32361133559)

*Corresponding authors, E-mail: pansk@ioz.ac.cn; zhanxj@ioz.ac.cn

include various physiological and behavioral changes (Altshuler & Dudley, 2006; Boyle, 2017; Ivy & Guglielmo, 2023), such as increased heart and respiration rates (Lague et al., 2017), elevated hemoglobin oxygen levels (Hu et al., 2022), and adjustments in flight duration to reduce energetic costs (Barve et al., 2016). Efficient energy regulation, such as optimized glycolytic pathways, is crucial for vertebrate adaptation to hypoxia (Ding et al., 2021; Lau et al., 2017; Murray, 2016; Ramirez et al., 2007). For instance, hexokinase 1 (*HK1*), encoding a rate-limiting glycolytic enzyme, has been shown to mediate hypoxia adaptation in Tibetan chickens (*Gallus gallus*) through *HIF-1*-dependent regulation (Tang et al., 2021). Nonetheless, most prior studies have focused on long-term adaptations in high-altitude species (Ivy & Guglielmo, 2023) or chronic hypoxia treatments (Ho et al., 2020), with acute hypoxic responses in wild birds remaining largely uncharacterized.

The saker falcon (*Falco cherrug*), a raptor bird species that has recently expanded its range into the Qinghai-Xizang Plateau (Hu et al., 2022; Pan et al., 2017), provides an ideal model for studying acute responses to plateau hypoxia. This species occupies a broad elevational gradient (4 000–6 000 m above sea level (a.s.l.)), with a core distribution at 4 000–5 000 m a.s.l. (Zhan et al., 2015). Previous research identified elevation-associated increases in expression of oxygen transport isoforms (e.g. *EPAS1*) in highland populations compared to low-altitude populations, indicating chronic genomic responses to hypoxic conditions (Pan et al., 2017). Given these observations, the present study compared the activity levels of saker falcons across two elevation bands (4 000–5 000 m and 5 000–6 000 m a.s.l.) and evaluated their physiological and transcriptional changes following acute hypoxia exposure. Results revealed significant suppression of glycolysis in blood cells, mediated by the down-regulation of the key glycolytic gene *HK1*. This may represent an adaptive strategy to optimize energy allocation, thereby supporting sustained foraging activity at higher altitudes. Furthermore, chromatin accessibility profiling identified two conserved avian-specific cis-regulatory elements within the *HK1* locus, potentially enabling rapid transcriptional modulation under hypoxic stress. These regulatory features may contribute to short-term hypoxia tolerance in recently established highland populations.

MATERIALS AND METHODS

Ethics

All experimental procedures were approved by the Animal Ethics Committee of the Institute of Zoology, Chinese Academy of Sciences (No. IOZ-IACUC-2021-077). The field study was approved by the Three-River-Source National Park Administration, Qinghai Province, China (No. 2022-189).

Activity tracking of saker falcons and upland buzzards

Tri-axial acceleration (ACC) data were collected using 15 g GSM transmitters (HQB2715L, Global Messenger Inc., China) attached to six juvenile saker falcons and four juvenile upland buzzards (*Buteo hemilasius*) in Qinghai Province (Supplementary Table S1). Each transmitter recorded ACC data every 10 min, capturing 7 s segments at a sampling frequency of 10 Hz. Movement intensity was quantified using overall dynamic body acceleration (ODBA), a well-established proxy for avian activity (Aikens et al., 2024; Pokrovsky et al., 2021). ODBA was calculated as the absolute sum of dynamic

acceleration components along all three axes, with dynamic acceleration obtained by subtracting smoothed static acceleration from raw acceleration data (Martín López et al., 2022).

Given that the falcons used in the hypoxia chamber study exhibited exclusively non-flight behaviors, activities with $ODBA \leq 0.15$ g were classified as non-flight behaviors and used as the focus for comparison with free-ranging sakers across different altitudes. Activities exceeding this threshold ($ODBA > 0.15$ g) were defined as flight behaviors. To assess the association between altitude and activity levels, Pearson correlation analyses were performed using ODBA values averaged over 30 min intervals. Corresponding altitude data were extracted for each interval (Supplementary Table S2), and Pearson correlation coefficients (r) were computed separately for saker falcons and upland buzzards.

Hypoxia exposure and physiological assessment

To investigate molecular and physiological responses to acute hypoxia, 27 pre-fledging saker falcons (aged 5–6 weeks) were obtained from artificial nests within an experimental grid in Madoi County, Qinghai Province, at an average altitude of 4 300 m a.s.l. To avoid pseudo replication, only one chick per nest was randomly selected for inclusion (Supplementary Table S3). Experiments were conducted at the Yellow River Source Wildlife Protection Research Station, Chinese Academy of Sciences.

Chicks were first acclimated for seven days under laboratory conditions mimicking native environmental parameters (air pressure: 62.1 kPa, partial oxygen pressure: 13.0 kPa, oxygen concentration: 20.9%, humidity: 50%, temperature: 15°C) based on the International Standard Atmosphere (ISA) model. During acclimation, each chick received 150 g of fresh beef daily and unlimited access to water. On day 8, 500–600 μ L of blood was collected from each chick to serve as the baseline control (natural environment (NE) group). Following baseline sampling, individuals were transferred to an oxygen chamber (ProOx-850, Shanghai Toward Intelligent Technology Co., Ltd., China) adjusted to simulate the partial oxygen pressure at 6 000 m a.s.l. (air pressure: 51.1 kPa, partial oxygen pressure: 10.7 kPa, oxygen concentration: 20.9%, humidity: 50%, temperature: 15°C). High-altitude hypobaric hypoxia was achieved by modulating air pressure within the sealed chamber, rather than adjusting oxygen concentration. Blood samples (700–800 μ L) were subsequently collected from three individuals at 0.5, 2, 4, 6, 12, and 24 h post-treatment exposure. An additional nine chicks were sampled after 72 h of hypoxia exposure, forming the simulated hypoxia (SH) group. For each sample, a 100 μ L aliquot was immediately preserved in RNA protect Animal Blood Tubes (Qiagen, Germany) and stored in liquid nitrogen for RNA extraction. The remaining blood was retained in EDTA tubes (BD, USA) for hematological assays, plasma isolation, and ATAC-seq. Upon completion of the experiment, all chicks were returned to their nests and remotely monitored on a daily basis until fledging. Phenotypic assessments conducted before and after treatment showed no adverse effects on the fledging success, survival, or developmental outcomes (Supplementary Table S4).

Physiological and biochemical measurements of blood samples

Blood samples from six individuals per group were analyzed

using an automated hematology analyzer (B412, Gaugene) to measure four hematological parameters, including total hemoglobin (HGB), hematocrit (HCT), mean corpuscular volume (MCV), and mean corpuscular hemoglobin (MCH). For each measurement, 20 μ L of whole blood was used for analysis. Samples were centrifuged at 1 000 \times g for 10 min at 4°C to isolate plasma. To quantify blood glucose levels, 50 μ L of whole blood was analyzed using a portable glucometer (Accu-Chek® Performa, Roche, Switzerland), previously validated for avian blood (Lieske et al., 2002; Mohsenzadeh et al., 2015). For each individual, three measurements were taken using separate test strips, and the average value was used for analysis. Because measurements were obtained from the same chicks before and after hypoxia treatment, paired *t*-tests were used to assess statistical significance. Furthermore, 50 μ L of plasma collected at baseline and 72 h post-treatment was used to determine concentrations of total triglycerides (TG), total cholesterol (TC), high-density lipoprotein cholesterol (HDL-C), and low-density lipoprotein cholesterol (LDL-C) using commercial assay kits (BioSino, Bio-technology and Science Inc., China).

Identification of differentially expressed genes (DEGs) and pathway enrichment analysis

Total RNA was extracted from blood samples using an RNeasy Protect Animal Blood Kit (Qiagen, Germany), then subjected to mRNA purification, library preparation, and sequencing following previously established protocols (Pan et al., 2017). Raw RNA sequencing (RNA-seq) data were processed using the analysis pipeline developed by Hu et al. (2022). Initial quality control was performed using FastQC (Andrews, 2010). Reads containing adapter sequences, over 10% ambiguous bases, or more than 50% low-quality bases (Phred score<10) were excluded. The remaining high-quality clean reads were aligned to the saker falcon reference genome (Zhan et al., 2013; Hu et al., 2022) using HISAT2 with default parameters (Kim et al., 2019). Gene annotations were merged using STRINGTIE v.1.2.0 with default settings (Pertea et al., 2015) to construct a comprehensive transcript reference. Gene expression levels were quantified with FeatureCounts (Liao et al., 2014) and normalized as fragments per kilobase of transcript per million mapped reads (FPKM) (Mortazavi et al., 2008). Principal component analysis (PCA) was performed using FactoMineR (Lê et al., 2008).

Differential gene expression was assessed using three statistical frameworks: DESeq2 (Love et al., 2014), edgeR (Robinson et al., 2010; Zhou et al., 2014), and limma (Ritchie et al., 2015; Smyth, 2004). Genes with a log fold change (\log_2FC)>1.5, false discovery rate (FDR)<0.05, and identified by at least two of the three methods were designated as DEGs for downstream analyses. Functional enrichment of DEGs was evaluated using Gene Ontology (GO) (Ashburner et al., 2000; Thomas et al., 2022) and Kyoto Encyclopedia of Genes and Genomes (KEGG) (Kanehisa & Goto, 2000) databases via the R package clusterProfiler v.4.0.5 (Wu et al., 2021). Enrichment significance was determined using the hypergeometric test with a threshold of P <0.05.

Identification of differential ATAC-seq peaks

ATAC-seq analysis was conducted on six blood samples—three collected prior to treatment and three collected at 72 h post-treatment. Whole blood was centrifuged at 800 \times g for 10 min at 4°C, with the resulting cell pellets washed with phosphate-buffered saline (PBS) before being

resuspended in cryopreservation medium (90% fetal bovine serum (FBS), 10% dimethyl sulfoxide (DMSO)) at a concentration of 1 μ L blood cells per 1 mL medium. Libraries were prepared using the Omni-ATAC protocol (Grandi et al., 2022). Briefly, nuclei were isolated with a commercial lysis buffer (Illumina, USA) and subjected to tagmentation using a Tn5 transposase mixture (Illumina, USA). Sequencing was performed on the Illumina NovaSeq 6000 platform (USA).

Raw ATAC-seq data underwent quality control using Trimmomatic with default parameters (Bolger et al., 2014). Clean reads were then aligned to the saker falcon reference genome using BWA (Li & Durbin, 2009). Reads with Phred scores <20 and duplicates were removed. Open chromatin regions (ATAC-seq peaks) were identified using MACS2 (Gaspar, 2018) with the parameters “-nomodel -f BAMPE -p 0.05”, and peaks detected in at least two samples were retained for further analysis. Differential ATAC-seq peaks, representing chromatin regions with significantly altered accessibility, were identified using DiffBind (Stark & Brown, 2011) with thresholds of P <0.05 and \log_2FC >1. Potential transcription factor binding sites (TFBSs) and transcription factors (TFs) within these differential peaks were predicted using AliBaba2 (Grabe, 2002).

Co-expression analysis

To investigate potential regulatory networks involving *HK1*, co-expression analysis was performed across the transcriptome. Pearson correlation coefficients were calculated between *HK1* expression and that of all other expressed genes to assess the strength and direction of linear associations (Obayashi & Kinoshita, 2009). Correlation coefficients near +1 or -1 indicated strong positive or negative relationships, respectively, while values close to 0 implied no correlation. Statistical significance was determined using two-tailed *t*-tests with a threshold of P <0.05.

Comparative genomic analysis of the differential *HK1* peak across vertebrate species

To assess the evolutionary conservation of the differential *HK1* ATAC-seq peak, a comparative genomic analysis was conducted across 30 representative vertebrate species, including four mammals, four amphibians, four reptiles, and 18 bird species (including five from Falconiformes, two from Charadriiformes, one from Caprimulgiformes, one from Psittaciformes, two from Pelecaniformes, two from Passeriformes, one from Columbiformes, one from Anseriformes, and three from Galliformes) (Supplementary Table S5). A 400 bp sequence spanning the differential peak identified in the SH group was queried against this database using the Discontiguous MegaBLAST function in BLAST v.2.17.0 with default parameters (Morgulis et al., 2008). Orthologous sequences were extracted and aligned using ClustalW v.2.1 with default settings (Larkin et al., 2007). Ancestral sequence reconstruction for the 18 avian species was performed using the codeml module within the PAML v.4.9 package under default parameters (Yang, 2007), enabling inference of conserved regulatory elements within the *HK1* locus.

Estimation of selection pressure in coding and non-coding regions

To assess the evolutionary constraints acting on the putative cis-regulatory region upstream of *HK1*, pairwise selection pressure analyses were performed between saker falcons and

chickens. A 400 bp non-coding sequence located upstream of the annotated saker *HK1* transcription start site was aligned with its orthologous genomic region in chicken using MAFFT v.7 under default parameters (Kato & Standley, 2013). The adjacent coding sequence (CDS) was also extracted and aligned using the same procedure.

Selection pressure on the non-coding region was quantified using KaKs_Calculator v.3.0 in non-coding mode, which estimates the nucleotide substitution rate (*Kn*) within the query region and normalizes it by the synonymous substitution rate (*Ks*) derived from adjacent CDS regions (Zhang, 2022). The resulting *Kn/Ks* ratio serves as an indicator of selective constraint, where values <1 suggest purifying selection, and values >1 indicate positive selection.

Statistical analysis

Paired *t*-tests were performed using GraphPad Prism v.8.0 (GraphPad Software Inc., USA) to determine the significance of changes in activity levels of tracked sakers before and after reaching altitudes of 5 000–6 000 m a.s.l. These tests were also used to assess the significance of physiological responses observed during the hypoxia exposure experiment.

RESULTS

Raptor birds maintained consistent activity levels across altitudinal gradients

GPS tracking of six juvenile saker falcons yielded 15 222 valid data points for non-flight behaviors and 6 197 data points for flight behaviors between 4 000 and 6 000 m a.s.l. These individuals spent over 95% of their time at altitudes between 4 000 and 5 000 m a.s.l., with only about 5% of observations recorded between 5 000 and 6 000 m a.s.l. Despite this uneven altitudinal distribution, non-flight activity levels showed no significant correlation with elevation ($r=0.194$, $P=3.563e-129$; Figure 1B). Flight behavior also remained stable across altitudes ($r=-0.157$, $P=1.342e-35$; Supplementary Figure S1). A similar trend was observed in sympatric upland buzzards, which exhibited sustained activity levels across different elevations ($r=0.266$, $P=6.171e-80$; Supplementary Figure S2).

Acute physiological responses to hypoxia treatment

Exposure to hypoxia simulating oxygen conditions at 6000 m a.s.l. for 72 h resulted in marked hematological changes. Notably, HGB levels increased by 16.6%, from 154.1 g/L to 179.6 g/L, while HCT increased from 35.90% to 43.48%. Moreover, MCV and MCH increased from 120.6 fL to 132.0 fL and from 49.96 pg to 57.04 pg, respectively ($P=0.006$, 0.030, 0.001 and 0.003, respectively; Figure 1C). Blood glucose levels rose transiently from 7.1 mmol/L at 0.5 h to 9.3 mmol/L at 12 h post-treatment and peaked at 10.5 mmol/L after 72 h ($P_{12h}=0.002$, $P_{24h}=0.033$, $P_{72h}=0.006$; Figure 1D). Among the four plasma lipid indices measured, only LDL-C showed a significant decrease from 3.5 mmol/L to 2.8 mmol/L ($P=0.049$), while HDL-C, TC, and TG remained unchanged ($P=0.180$, 0.337, and 0.166, respectively, Figure 1E).

Blood transcriptomic response to hypoxia treatment

RNA-seq yielded an average of 10 Gb of high-quality data per individual, with over 96% of reads mapping to the reference genome (Supplementary Table S6). An average of 8 016 genes per sample was detected with *FPKM*>1. The PCA results revealed a clear separation between control and

hypoxia-treated groups (Figure 2A). Differential expression analysis identified 1 219 DEGs—including 659 up-regulated and 560 down-regulated in the hypoxia-treated group—consistently detected by at least two of the three independent methods (Figure 2B, C). KEGG pathway enrichment analysis revealed that up-regulated genes were associated with pathways such as “aldosterone-regulated sodium reabsorption” and “fatty acid elongation” (Supplementary Table S7). In contrast, the most significantly down-regulated pathway was “glycolysis/gluconeogenesis” (Figure 2D; Supplementary Table S8), with reduced expression of multiple genes involved in this pathway, including *HK1*, 6-phosphofructokinase I (*pfkA*), aldolase (*ALDO*), fructose-bisphosphate A, glyceraldehyde-3-phosphate dehydrogenase (*GAPDH*), and enolase 1 (*ENO1*) (Supplementary Table S9). Notably, *HK1*, a critical upstream regulator of glycolytic flux, showed the most pronounced suppression, with a 1.6-fold reduction in expression under hypoxia. In addition, GO enrichment analysis revealed significant overrepresentation of terms such as “cytokine binding”, “kinase regulator activity” and “phospholipase inhibitor activity”, suggesting that immune signaling and regulatory responses were also engaged under acute hypoxic stress (Supplementary Table S10).

Differential chromatin accessibility in the *HK1* region under hypoxia

ATAC-seq generated an average of 4.56 Gb of clean data per individual across six saker falcons (three control and three hypoxia-treated) (Supplementary Table S11). A total of 61 479 accessible chromatin regions (peaks) were identified, of which 46 470 exhibited significant differential accessibility between groups. Within the *HK1* locus, two peaks were detected. Among them, only the peak located at Chr (chromosome) 10: 19 125 856–19 126 256 showed a significant difference ($P<0.05$), with increased accessibility in the hypoxia-treated group (Figure 3A).

Co-expressed genes and putative TFBSs for *HK1*

Co-expression analysis identified 2 254 genes positively correlated with *HK1* and 1 069 genes negatively correlated with *HK1* (Supplementary Table S12). Within the differentially accessible *HK1* peak, 27 TFBSs corresponding to 20 TFs were predicted (Supplementary Table S13). In comparison, the other *HK1*-associated ATAC-seq peak contained 56 TFBSs associated with 55 TFs (Supplementary Table S14). Notably, among the 20 TFs predicted within the differential peak, NR3C1, with two potential TFBSs, was the only TF exhibiting a significant negative correlation with *HK1* ($r=-0.59$, $P=0.026$), suggesting a potential role in transcriptional repression of *HK1* under hypoxia (Figure 3A).

Conservation of the differential *HK1* ATAC-seq peak across bird species

Comparative genomic analysis of the 400 bp sequence spanning the differential *HK1* ATAC-seq peak across 18 avian and 12 non-avian vertebrate species (including mammals, amphibians, and reptiles) revealed that this region is unique to birds and absent in other evolutionary lineages. Among avian genomes, this element displayed over 90% sequence identity (Figure 3B). Ancestral sequence reconstruction suggested the NR3C1 binding sites within this region likely originated in the common ancestor of the avian crown group. To evaluate selective pressure, a pairwise *Kn/Ks* analysis was conducted

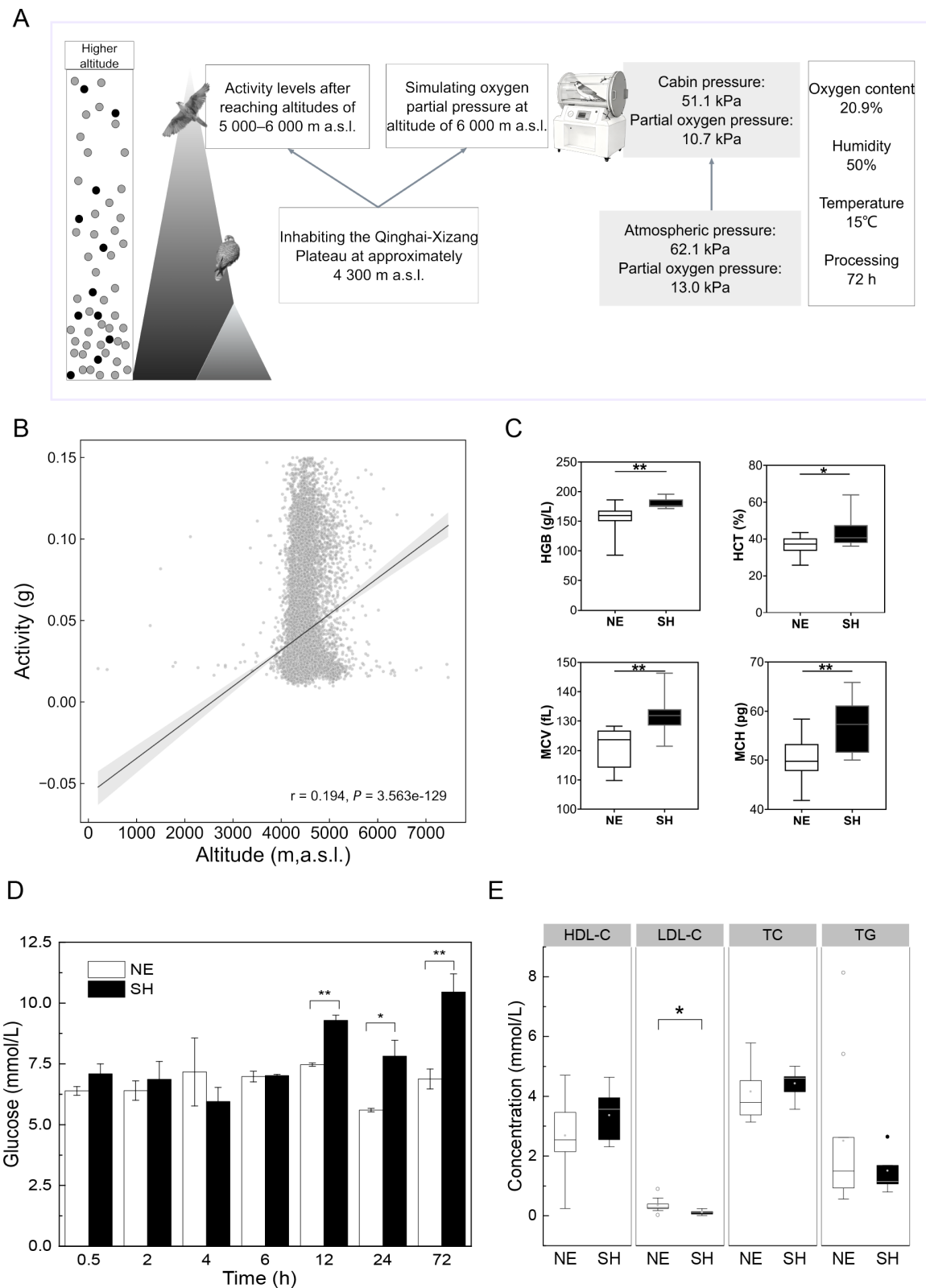


Figure 1 Analysis of activity and physiological responses in saker falcons

A: Schematic overview of the experimental design, including simulation of hypoxic conditions at 6 000 m a.s.l. and the natural habitat on the Qinghai-Xizang Plateau (approximately 4 300 m a.s.l.). Black dots represent oxygen molecules; gray dots represent other atmospheric components besides oxygen. B: Relationship between half-hourly mean overall dynamic body acceleration (ODBA, g) and altitude ($n=6$). C: Comparisons of hematological indices, including total hemoglobin (HGB, g/dL), hematocrit (HCT, %), mean corpuscular volume (MCV, fL), and mean corpuscular hemoglobin (MCH, pg) between the natural environment (NE) and simulated hypoxia (SH) groups ($n=9$). D: Time-series analysis of blood glucose concentrations (mmol/L) between the NE and SH groups ($n=3$). E: Comparisons of plasma lipid profiles, including high-density lipoprotein cholesterol (HDL-C), low-density lipoprotein cholesterol (LDL-C), total cholesterol (TC), and total triglycerides (TG) (mmol/L) between NE and SH groups ($n=9$). *: $P<0.05$; **: $P<0.01$, paired t -tests.

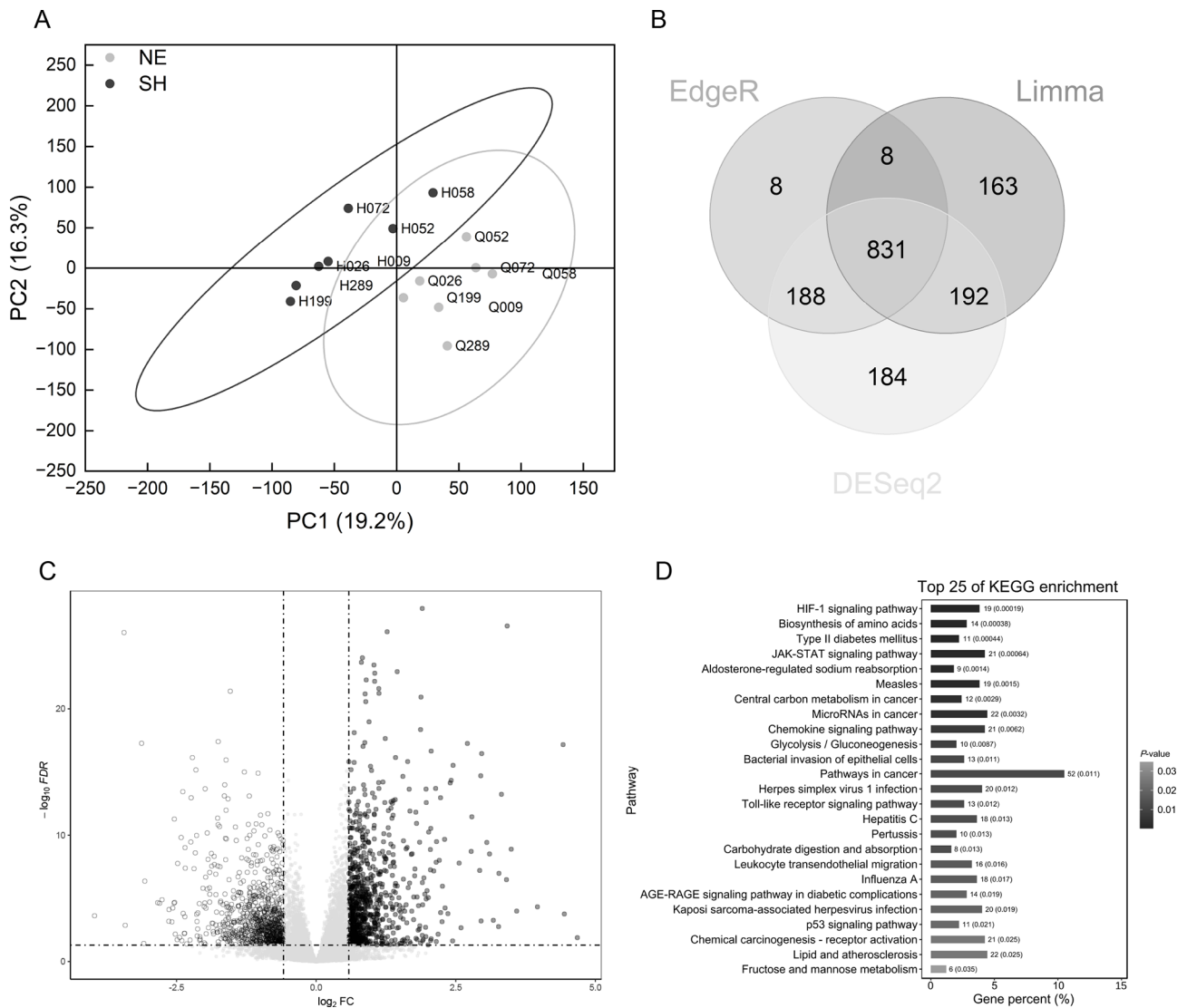


Figure 2 Comparison of blood transcriptomes between the hypoxia-treated and control groups

A: PCA analysis on studied individuals based on gene expression profiles. B: Venn diagram of DEGs identified by three different methods. C: Volcano plot of DEGs in hypoxia-treated group generated from DESeq2 analysis, where black dots represent up-regulated genes and black circles represent down-regulated genes. D: KEGG pathway enrichment analysis on DEGs down-regulated in the SH group.

between the saker falcon and chicken. The focal non-coding region yielded a Kn/Ks ratio of 0.097, indicative of strong purifying selection. Similarly, the adjacent *HK1* coding sequence exhibited a Kn/Ks ratio of 0.045. These results suggest that both the regulatory element and coding region of *HK1* are under strong evolutionary constraint, underscoring the functional relevance of this conserved upstream motif in avian hypoxia adaptation.

DISCUSSION

This study observed consistent activity levels in saker falcons and upland buzzards across their altitudinal ranges on the Qinghai-Xizang Plateau, indicating behavioral resilience to hypobaric hypoxia. Sustaining movement under such oxygen-limited conditions typically requires elevated aerobic capacity or increased energy turnover (Scott & Milsom, 2006; Storz et al., 2010). High basal metabolic rates may facilitate these processes by supporting extended flight performance essential for foraging efficiency and meeting the increased energy demands of cold, hypoxic environments (Gutierrez-

Pinto, 2021; Capainolo & Butler, 2010; Pan et al., 2017). Notably, this sustained activity contrasts with that of non-raptorial vertebrates—such as high-altitude passerines and small mammals—which often exhibit reduced activity at elevation, likely as an energy-conservation strategy (Uno et al., 2020; Xiong et al., 2020; Zhou et al., 2011).

The hypoxic conditions of the Qinghai-Xizang Plateau, characterized by significantly reduced oxygen availability, impose substantial physiological challenges on aerobic organisms (Zhao et al., 2024). In high-altitude mammals, such as yaks and rodents, physiological compensation is achieved through increased red blood cell counts and elevated hemoglobin concentrations, enhancing systemic oxygen delivery (Arias-Reyes et al., 2021; Ayalew et al., 2021; Gassmann et al., 2019). However, most comparative studies of highland adaptations have focused on population-level divergence, with limited attention to acute, within-species physiological plasticity. In the present study, acute exposure of pre-fledging saker falcons to simulated hypoxia elicited a significant increase in hemoglobin concentration, consistent with the Andean-type adaptation observed in human

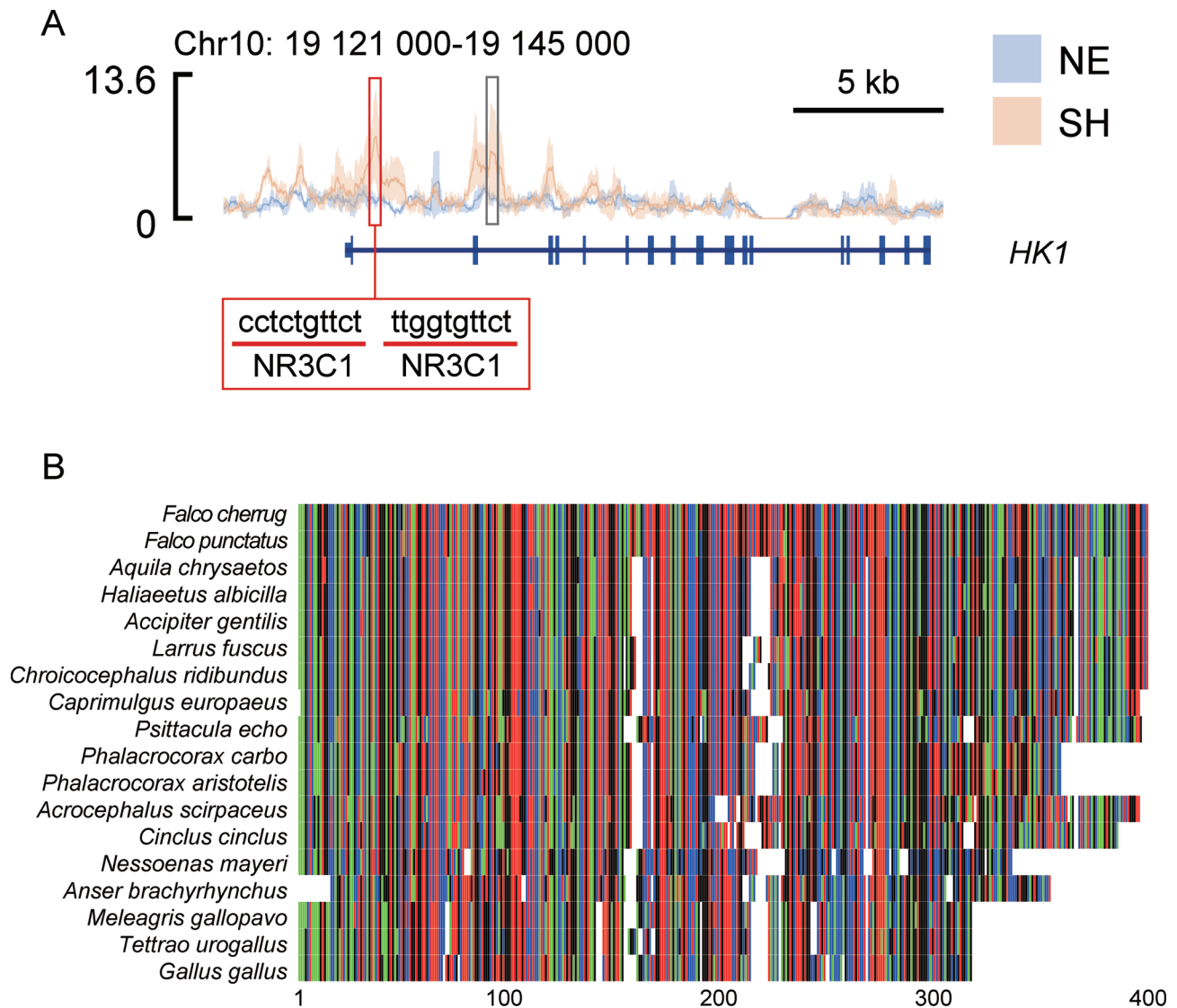


Figure 3 Comparative chromatin accessibility and sequence conservation in the *HK1* gene

A: ATAC-seq profiling identified two peaks across the *HK1* gene region. The peak with significantly altered accessibility between the control (NE) and hypoxia-treated (SH) groups is outlined in red, while the peak without significant differences is outlined in gray. Two predicted NR3C1 binding sites are highlighted in red. Gene structure is shown in blue, with a rectangle representing the CDS and a shorter block indicating the UTR region. B: Alignment of homologous DNA sequences spanning the differential ATAC-seq peak in *HK1* across 18 avian species. Nucleotide bases are color-coded: A (green), T (red), C (blue), and G (black), with alignment gaps shown as white spaces.

highlanders, in which elevated hemoglobin enhances oxygen transport under chronic hypoxia (Beall, 2007). Notably, red blood cell counts remained unchanged ($P=0.745$; Supplementary Figure S3), suggesting that sakers employ a species-specific strategy to avoid increased blood viscosity (Yu et al., 2024). This unique physiological flexibility offers new insights into oxygen transport mechanisms in hypoxic environments and highlights a previously underappreciated facet of hypoxia tolerance in high-altitude raptors.

Saker falcons exhibited marked metabolic responses to acute hypoxia, including a 47.9% increase in blood glucose concentrations following 72 h of exposure. Transcriptomic profiling of peripheral blood cells revealed significant down-regulation of *HK1*, a rate-limiting gene in the glycolytic pathway, indicating suppressed glycolytic flux in the hematopoietic compartment. This repression may reflect a systemic regulatory mechanism that limits glucose catabolism in peripheral tissues to preserve substrate availability for metabolically critical organs during oxygen deprivation.

Glucose redistribution under hypoxic stress has been reported across vertebrate taxa. In rats (*Rattus norvegicus*) subjected to focal cerebral ischemia, expression of *GLUT1* and several glycolytic enzymes has been shown to increase significantly from 7.5 h to 24 h post-insult (Bergeron et al., 2000). Similarly, high-altitude deer mice (*Peromyscus maniculatus*) show elevated hexokinase activity in skeletal muscles compared to their lowland conspecifics, suggesting muscle-specific enhancement of glycolysis to meet increased ATP demands (Garrett et al., 2024). Given that glucose is the primary energy substrate for the brain, increased cerebral glucose availability under hypoxia is likely critical for preserving neural function and sustaining activity (Magistretti & Allaman, 2022; von Eugen et al., 2022). Moreover, glycolysis also generates ATP more rapidly than lipid metabolism, making it particularly advantageous for fueling short bursts of high-intensity exertion such as rapid flight maneuvers during hunting (Jenni-Eiermann & Srygley, 2017). These findings collectively support the hypothesis that sakers modulate glucose

metabolism during acute hypoxia to prioritize energy delivery to vital organs and tissues with immediate metabolic demands. Due to conservation constraints—*F. cherrug* is listed as endangered on the IUCN Red List—it remains ethically and logistically difficult to obtain internal organs such as liver, muscle, or brain for comprehensive transcriptomic or metabolomic analyses. While blood provides a minimally invasive alternative that enables insight into systemic responses, future studies aiming to elucidate tissue-specific glucose reallocation mechanisms under hypoxia would benefit from the use of non-threatened avian models that permit multi-tissue sampling.

Although studies have highlighted the role of gene expression divergence and *cis*-regulatory elements in avian high-altitude adaptation (e.g., Hu et al., 2022; Pan et al., 2017), the contribution of trans-acting regulatory factors remains underexplored. To elucidate the upstream regulatory mechanisms governing *HK1* expression under hypoxic stress, integrative ATAC-seq and expression correlation analyses were performed, identifying the glucocorticoid receptor NR3C1 as a potential regulator. Evolutionary analysis revealed that the NR3C1-*HK1* regulatory axis is unique to avian genomes, suggesting its lineage-specific evolution approximately 115 million years ago (Zhang et al., 2014). Comparative genomic screening of 30 representative vertebrate genomes spanning birds, mammals, reptiles, and amphibians identified a 400 bp upstream element within the *HK1* locus that was uniquely conserved in birds and completely absent in non-avian vertebrates, with no evidence of partial or syntenic homology in either placental mammals (e.g., *Homo sapiens*, *Mus musculus*) or non-avian reptiles (e.g., *Chrysemys picta*, *Anolis carolinensis*), even under relaxed BLAST thresholds ($E\text{-value} < 1e^{-5}$). These findings suggest a *de novo* origin of this element in the avian lineage, possibly via sequence turnover, regulatory capture, or transposable element duplication—mechanisms previously proposed for lineage-specific regulatory innovation (Feschotte, 2008; Villar et al., 2015). The high sequence identity (>90%) observed across the 18 avian species, coupled with the strong signature of purifying selection ($K_n/K_s = 0.097$), indicates functional constraint following its emergence, likely contributing to conserved regulatory control of *HK1* expression.

NR3C1 binds to glucocorticoid response elements (GREs) and exerts either transcriptional activation or repression depending on chromatin context and co-regulatory partner recruitment. In the presence of co-activators such as SRC-1 or CBP/p300, NR3C1 promotes the expression of gluconeogenic genes including *PEPCK* and *G6Pase* (Beato & Klug, 2000; Reddy et al., 2009). Conversely, binding to negative GREs (nGREs) or other transcription factors such as AP-1 or NF- κ B enables NR3C1 to recruit co-repressors, such as NCoR and HDACs, to mediate transcriptional repression (Oakley & Cidlowski, 2013; Surjit et al., 2011). We propose that NR3C1 interacts with the avian-specific *cis*-regulatory element to repress *HK1* expression in blood cells under acute hypoxia, thereby facilitating glucose redistribution toward energetically demanding organs. This regulatory mechanism may have contributed to hypoxia resilience in early avian lineages, potentially driving their diversification during extreme global environmental changes, such as the Cretaceous-Paleogene mass extinction (Wilson et al., 2012). Although strong sequence conservation and evidence of purifying selection at the *HK1* upstream element support its functional relevance,

direct validation of NR3C1-mediated repression under hypoxia remains unresolved. Experimental approaches, such as reporter gene assays in avian cell systems or CRISPR-based perturbation, will be critical to establishing causality between chromatin accessibility, NR3C1 binding, and *HK1* transcriptional regulation.

As rising global temperatures accelerate altitudinal range shifts in Qinghai-Xizang Plateau birds (Meng et al., 2021; Parmesan & Yohe, 2003), the capacity to withstand intensifying hypoxia is becoming increasingly vital. The acute physiological responses identified in this study, including hemoglobin elevation, glucose reallocation via blood *HK1* down-regulation, and avian-specific regulatory adaptations at the *HK1* locus, may underlie sustained aerobic performance and predatory efficiency at higher elevations. These mechanistic insights underscore the potential for molecular and regulatory traits to influence ecological resilience and may refine projections of species vulnerability under future climate scenarios.

CONCLUSIONS

This study identified a potential regulatory mechanism by which the NR3C1-*HK1* regulatory axis modulates glucose allocation in blood cells to support sustained activity under acute hypoxia at high-altitude environments. Using the saker falcon as a model, evidence suggests that repression of *HK1* expression may function as a strategic metabolic adjustment, facilitating glucose redistribution to oxygen-sensitive tissues during exposure to low-oxygen conditions. Although these findings shed light on a previously unrecognized component of avian hypoxic response, further research is required to explore its involvement in chronic adaptation to hypoxia. Broader investigation into additional metabolic pathways and their contributions to resource allocation under hypoxic stress would provide a more comprehensive understanding of avian adaptation to extreme environments. In conclusion, this study integrated physiological, transcriptomic, and chromatin accessibility data to reveal blood-based responses to acute hypoxia in Qinghai-Xizang Plateau birds. Altered hematological parameters and glycolytic gene repression point to flexible metabolic strategies that may sustain activity under oxygen-limited conditions. These findings enhance understanding of altitude adaptation and inform predictions of avian resilience to climate-driven elevational shifts.

DATA AVAILABILITY

All data reported in this study have been deposited in the NCBI database under BioProjectID PRJNA1269714; GSA database (<https://ngdc.cnca.ac.cn/gsa/>) under accession numbers CRA019903 (RNA-seq) and CRA019904 (ATAC-seq); and Science Data Bank (<https://www.scidb.cn/>) under DOI: 10.57760/sciencedb.24680. The saker falcon reference genome is available in the CNCB database under accession number GWHBOUP00000000.

SUPPLEMENTARY DATA

Supplementary data to this article can be found online.

COMPETING INTERESTS

The authors declare that they have no competing interests.

AUTHORS' CONTRIBUTIONS

X.J.Z. and S.K.P. designed the research. W.W., S.K.P., J.F.C., and X.J.Z. wrote the manuscript. W.W. performed sampling, experiments, and data

analysis. X.H.Z. and L.H. analyzed the ATAC-seq data. W.W. and X.H.Z. drew the figures. F.F.D. assisted with blood sample collection and glucose content measurement. Z.R.G. provided the saker tracking data. Z.Z.L. assisted with field sample collection and experiments. All authors read and approved the final version of the manuscript.

ACKNOWLEDGMENTS

We thank Fan Li (Institute of Zoology, Chinese Academy of Sciences), Xue-Jiao Yang, and Jin-Biao Sun (Institute of Zoology, Chinese Academy of Sciences) for their assistance with sample collection in the field, and Dr. Yuan-Yuan Wang (Shanghai Institute of Immunity and Infection, Chinese Academy of Sciences) for help with initial ATAC-seq processing.

REFERENCES

- Aikens EO, Nourani E, Fiedler W, et al. 2024. Learning shapes the development of migratory behavior. *Proceedings of the National Academy of Sciences of the United States of America*, **121**(12): e2306389121.
- Altshuler DL, Dudley R. 2006. The physiology and biomechanics of avian flight at high altitude. *Integrative and Comparative Biology*, **46**(1): 62–71.
- Andrews S. 2010. FastQC: a quality control tool for high throughput sequence data. <https://www.scienceopen.com/document?vid=44afede7-32e8-471e-9ad3-83d382b0f62a>
- Arias-Reyes C, Soliz J, Joseph V. 2021. Mice and rats display different ventilatory, hematological, and metabolic features of acclimatization to hypoxia. *Frontiers in Physiology*, **12**: 647822.
- Ashburner M, Ball CA, Blake JA, et al. 2000. Gene Ontology: tool for the unification of biology. *Nature Genetics*, **25**(1): 25–29.
- Ayalew W, Chu M, Liang CN, et al. 2021. Adaptation mechanisms of yak (*Bos grunniens*) to high-altitude environmental stress. *Animals*, **11**(8): 2344.
- Barve S, Dhondt AA, Mathur VB, et al. 2016. Life-history characteristics influence physiological strategies to cope with hypoxia in Himalayan birds. *Proceedings of the Royal Society B: Biological Sciences*, **283**(1843): 20162201.
- Beall CM. 2007. Two routes to functional adaptation: Tibetan and Andean high-altitude natives. *Proceedings of the National Academy of Sciences of the United States of America*, **104**(suppl_1): 8655–8660.
- Beato M, Klug J. 2000. Steroid hormone receptors: an update. *Human Reproduction Update*, **6**(3): 225–236.
- Bergeron M, Gidday JM, Yu AY, et al. 2000. Role of hypoxia-inducible factor-1 in hypoxia-induced ischemic tolerance in neonatal rat brain. *Annals of Neurology*, **48**(3): 285–296.
- Bolger AM, Lohse M, Usadel B. 2014. Trimmomatic: a flexible trimmer for Illumina sequence data. *Bioinformatics*, **30**(15): 2114–2120.
- Boyle WA. 2017. Altitudinal bird migration in North America. *The Auk*, **134**(2): 443–465.
- Capainolo P, Butler CA. 2010. How Fast Can a Falcon Dive? Fascinating Answers to Questions About Birds of Prey. New Brunswick: Rutgers University Press.
- Collier RJ, Gebremedhin KG. 2015. Thermal biology of domestic animals. *Annual Review of Animal Biosciences*, **3**(1): 513–532.
- Ding BY, Zhao YL, Sun YF, et al. 2021. Coping with extremes: lowered myocardial phosphofructokinase activities and glucose content but increased fatty acids content in highland Eurasian tree sparrows. *Avian Research*, **12**(1): 44.
- Feschotte C. 2008. Transposable elements and the evolution of regulatory networks. *Nature Reviews Genetics*, **9**(5): 397–405.
- Garrett EJ, Prasad SK, Schweizer RM, et al. 2024. Evolved changes in phenotype across skeletal muscles in deer mice native to high altitude. *American Journal of Physiology-Regulatory, Integrative and Comparative Physiology*, **326**(4): R297–R310.
- Gaspar JM. 2018. Improved peak-calling with MACS2. *BioRxiv*, doi: <https://doi.org/10.1101/496521>.
- Gassmann M, Mairbörl H, Livshits L, et al. 2019. The increase in hemoglobin concentration with altitude varies among human populations. *Annals of the New York Academy of Sciences*, **1450**(1): 204–220.
- Grabe N. 2002. AliBaba2: context specific identification of transcription factor binding sites. *In Silico Biology*, **2**(1): S1–S15.
- Grandi FC, Modi H, Kampman L, et al. 2022. Chromatin accessibility profiling by ATAC-seq. *Nature Protocols*, **17**(6): 1518–1552.
- Gutierrez-Pinto N, Londoño GA, Chappell MA, et al. 2021. A test of altitude-related variation in aerobic metabolism of Andean birds. *Journal of Experimental Biology*, **224**(11): 1–6.
- Ho WC, Li DY, Zhu Q, et al. 2020. Phenotypic plasticity as a long-term memory easing readaptations to ancestral environments. *Science Advances*, **6**(21): eaba3388.
- Hu L, Long J, Lin Y, et al. 2022. Arctic introgression and chromatin regulation facilitated rapid Qinghai-Tibet Plateau colonization by an avian predator. *Nature Communications*, **13**(1): 6413.
- Ivy CM, Guglielmo CG. 2023. Migratory songbirds exhibit seasonal modulation of the oxygen cascade. *Journal of Experimental Biology*, **226**(17): jeb245975.
- Jenni-Eiermann S, Srygley RB. 2017. Physiological aeroecology: anatomical and physiological adaptations for flight. In: Chilson PB, Frick WF, Kelly JF, et al. *Aeroecology*. Cham: Springer, 87–118.
- Jiang DC, Zhao XM, López-Pujol J, et al. 2023. Effects of climate change and anthropogenic activity on ranges of vertebrate species endemic to the Qinghai-Tibet Plateau over 40 years. *Conservation Biology*, **37**(4): e14069.
- Kanehisa M, Goto S. 2000. KEGG: Kyoto encyclopedia of genes and genomes. *Nucleic Acids Research*, **28**(1): 27–30.
- Katoh K, Standley DM. 2013. MAFFT multiple sequence alignment software version 7: improvements in performance and usability. *Molecular Biology and Evolution*, **30**(4): 772–780.
- Kim D, Paggi JM, Park C, et al. 2019. Graph-based genome alignment and genotyping with HISAT2 and HISAT-genotype. *Nature Biotechnology*, **37**(8): 907–915.
- Lague SL, Chua B, Alza L, et al. 2017. Divergent respiratory and cardiovascular responses to hypoxia in bar-headed geese and Andean birds. *Journal of Experimental Biology*, **220**(22): 4186–4194.
- Larkin MA, Blackshields G, Brown NP, et al. 2007. Clustal W and Clustal X version 2.0. *Bioinformatics*, **23**(21): 2947–2948.
- Lau DS, Connaty AD, Mahalingam S, et al. 2017. Acclimation to hypoxia increases carbohydrate use during exercise in high-altitude deer mice. *American Journal of Physiology-Regulatory, Integrative and Comparative Physiology*, **312**(3): R400–R411.
- Lê S, Josse J, Husson F. 2008. FactoMineR: an R package for multivariate analysis. *Journal of Statistical Software*, **25**(1): 1–18.
- Li B, Liang CB, Song PF, et al. 2023. Threatened birds face new distribution under future climate change on the Qinghai-Tibet Plateau (QTP). *Ecological Indicators*, **150**: 110217.
- Li H, Durbin R. 2009. Fast and accurate short read alignment with Burrows–Wheeler transform. *Bioinformatics*, **25**(14): 1754–1760.
- Liao Y, Smyth GK, Shi W. 2014. featureCounts: an efficient general purpose program for assigning sequence reads to genomic features. *Bioinformatics*, **30**(7): 923–930.
- Lieske CL, Ziccardi MH, Mazet JAK, et al. 2002. Evaluation of 4 handheld blood glucose monitors for use in seabird rehabilitation. *Journal of Avian Medicine and Surgery*, **16**(4): 277–285.
- Love MI, Huber W, Anders S. 2014. Moderated estimation of fold change and dispersion for RNA-seq data with DESeq2. *Genome Biology*, **15**(12): 550.
- Magistretti PJ, Allaman I. 2022. Brain energy and metabolism. In: Pfaff DW, Volkow ND, Rubenstein JL. *Neuroscience in the 21st Century: From Basic*

to Clinical. Cham: Springer, 2197–2227.

Martín López LM, de Soto NA, Madsen PT, et al. 2022. Overall dynamic body acceleration measures activity differently on large versus small aquatic animals. *Methods in Ecology and Evolution*, **13**(2): 447–458.

Meng N, Yang YZ, Zheng H, et al. 2021. Climate change indirectly enhances sandstorm prevention services by altering ecosystem patterns on the Qinghai-Tibet Plateau. *Journal of Mountain Science*, **18**(7): 1711–1724.

Mohsenzadeh MS, Zaeemi M, Razmyar J, et al. 2015. Comparison of a point-of-care glucometer and a laboratory autoanalyzer for measurement of blood glucose concentrations in domestic pigeons (*Columba livia domestica*). *Journal of Avian Medicine and Surgery*, **29**(3): 181–186.

Morgulis A, Coulouris G, Raytselis Y, et al. 2008. Database indexing for production MegaBLAST searches. *Bioinformatics*, **24**(16): 1757–1764.

Mortazavi A, Williams BA, McCue K, et al. 2008. Mapping and quantifying mammalian transcriptomes by RNA-seq. *Nature Methods*, **5**(7): 621–628.

Murray AJ. 2016. Energy metabolism and the high-altitude environment. *Experimental Physiology*, **101**(1): 23–27.

Oakley RH, Cidlowski JA. 2013. The biology of the glucocorticoid receptor: new signaling mechanisms in health and disease. *Journal of Allergy and Clinical Immunology*, **132**(5): 1033–1044.

Obayashi T, Kinoshita K. 2009. Rank of correlation coefficient as a comparable measure for biological significance of gene coexpression. *DNA Research*, **16**(5): 249–260.

Pan SK, Zhang TZ, Rong ZQ, et al. 2017. Population transcriptomes reveal synergistic responses of DNA polymorphism and RNA expression to extreme environments on the Qinghai-Tibetan Plateau in a predatory bird. *Molecular Ecology*, **26**(11): 2993–3010.

Parmesan C, Yohe G. 2003. A globally coherent fingerprint of climate change impacts across natural systems. *Nature*, **421**(6918): 37–42.

Pertea M, Pertea GM, Antonescu CM, et al. 2015. StringTie enables improved reconstruction of a transcriptome from RNA-seq reads. *Nature Biotechnology*, **33**(3): 290–295.

Pokrovsky I, Kölsch A, Sherub S, et al. 2021. Longer days enable higher diurnal activity for migratory birds. *Journal of Animal Ecology*, **90**(9): 2161–2171.

Ramirez JM, Folkow LP, Blix AS. 2007. Hypoxia tolerance in mammals and birds: from the wilderness to the clinic. *Annual Review of Physiology*, **69**(1): 113–143.

Reddy TE, Pauli F, Sprouse RO, et al. 2009. Genomic determination of the glucocorticoid response reveals unexpected mechanisms of gene regulation. *Genome Research*, **19**(12): 2163–2171.

Ritchie ME, Phipson B, Wu D, et al. 2015. limma powers differential expression analyses for RNA-sequencing and microarray studies. *Nucleic Acids Research*, **43**(7): e47.

Robinson MD, McCarthy DJ, Smyth GK. 2010. edgeR: a Bioconductor package for differential expression analysis of digital gene expression data. *Bioinformatics*, **26**(1): 139–140

Scott GR, Milsom WK. 2006. Flying high: a theoretical analysis of the factors limiting exercise performance in birds at altitude. *Respiratory Physiology & Neurobiology*, **154**(1-2): 284–301.

Smyth GK. 2004. Linear models and empirical bayes methods for assessing differential expression in microarray experiments. *Statistical Applications in Genetics and Molecular Biology*, **3**(1): 1–25.

Stark R, Brown G. 2011. *DiffBind*: differential binding analysis of ChIP-seq peak data. *R Package Version*, **100**(43): 1–12.

Storz JF, Scott GR, Cheviron ZA. 2010. Phenotypic plasticity and genetic adaptation to high-altitude hypoxia in vertebrates. *Journal of Experimental Biology*, **213**(24): 4125–4136.

Surjit M, Ganti KP, Mukherji A, et al. 2011. Widespread negative response elements mediate direct repression by agonist- liganded glucocorticoid receptor. *Cell*, **145**(2): 224–241.

Tang QG, Xu QQ, Ding C, et al. 2021. HIF-1 regulates energy metabolism of the Tibetan chicken brain during embryo development under hypoxia. *American Journal of Physiology-Regulatory, Integrative and Comparative Physiology*, **320**(5): R704–R713.

Thomas PD, Ebert D, Muruganujan A, et al. 2022. PANTHER: making genome-scale phylogenetics accessible to all. *Protein Science*, **31**(1): 8–22.

Uno T, Hasegawa T, Horiuchi M. 2020. Combined stimuli of cold, hypoxia, and dehydration status on body temperature in rats: a pilot study with practical implications for humans. *BMC Research Notes*, **13**(1): 530.

Villar D, Berthelot C, Aldridge S, et al. 2015. Enhancer evolution across 20 mammalian species. *Cell*, **160**(3): 554–566

von Eugen K, Endepols H, Drzezga A, et al. 2022. Avian neurons consume three times less glucose than mammalian neurons. *Current Biology*, **32**(19): 4306–4313. e4.

Wilson GP, Evans AR, Corfe IJ, et al. 2012. Adaptive radiation of multituberculate mammals before the extinction of dinosaurs. *Nature*, **483**(7390): 457–460.

Wu, T., Hu, E., Xu, S., et al. 2021. clusterProfiler 4.0: A universal enrichment tool for interpreting omics data. *Innovation*, **2**(3): 100141.

Xiong Y, Fan LQ, Hao Y, et al. 2020. Physiological and genetic convergence supports hypoxia resistance in high-altitude songbirds. *PLoS Genetics*, **16**(12): e1009270.

Yang Z. 2007. PAML 4: phylogenetic analysis by maximum likelihood. *Molecular Biology and Evolution*, **24**(8): 1586–1591.

Yu S, Ye Y, Wuren T, et al. 2024. Alteration in the number, morphology, function, and metabolism of erythrocytes in high-altitude polycythemia. *Frontiers in Physiology*, **15**(2024): 13.

Zhan XJ, Dixon A, Batbayar N, et al. 2015. Exonic versus intronic SNPs: contrasting roles in revealing the population genetic differentiation of a widespread bird species. *Heredity*, **114**(1): 1–9.

Zhan XJ, Pan SK, Wang JY, et al. 2013. Peregrine and saker falcon genome sequences provide insights into evolution of a predatory lifestyle. *Nature Genetics*, **45**(5): 563–566.

Zhang GJ, Li C, Li QY, et al. 2014. Comparative genomics reveals insights into avian genome evolution and adaptation. *Science*, **346**(6215): 1311–1320.

Zhang, Z. 2022. KaKs_Calculator 3.0: calculating selective pressure on coding and non-coding sequences. *Genomics, Proteomics and Bioinformatics*, **20**(3): 536-540.

Zhao PF, Li SB, He ZH, et al. 2024. Physiological and genetic basis of high-altitude indigenous animals' adaptation to hypoxic environments. *Animals*, **14**(20): 3031.

Zhou QQ, Yang DZ, Luo YJ, et al. 2011. Over-starvation aggravates intestinal injury and promotes bacterial and endotoxin translocation under high-altitude hypoxic environment. *World Journal of Gastroenterology*, **17**(12): 1584–1593.

Zhou XB, Lindsay H, Robinson MD. 2014. Robustly detecting differential expression in RNA sequencing data using observation weights. *Nucleic Acids Research*, **42**(11): e91.